

Sensory Rhodopsin II from the Haloalkaliphilic *Natronobacterium pharaonis*: Light-Activated Proton Transfer Reactions

G. Schmies,* B. Lüttenberg,* I. Chizhov,* M. Engelhard,* A. Becker,[†] and E. Bamberg[†]

*Max-Planck-Institut für Molekulare Physiologie, D-44227 Dortmund, Germany; and [†]Max-Planck-Institut für Biophysik, D-60596 Frankfurt/Main, Germany

ABSTRACT In the present work the light-activated proton transfer reactions of sensory rhodopsin II from *Natronobacterium pharaonis* (pSRII) and those of the channel-mutants D75N-pSRII and F86D-pSRII are investigated using flash photolysis and black lipid membrane (BLM) techniques. Whereas the photocycle of the F86D-pSRII mutant is quite similar to that of the wild-type protein, the photocycle of D75N-pSRII consists of only two intermediates. The addition of external proton donors such as azide, or in the case of F86D-pSRII, imidazole, accelerates the reprotonation of the Schiff base, but not the turnover. The electrical measurements prove that pSRII and F86D-pSRII can function as outwardly directed proton pumps, whereas the mutation in the extracellular channel (D75N-pSRII) leads to an inwardly directed transient current. The almost negligible size of the photostationary current is explained by the long-lasting photocycle of about a second. Although the M decay, but not the photocycle turnover, of pSRII and F86D-pSRII is accelerated by the addition of azide, the photostationary current is considerably increased. It is discussed that in a two-photon process a late intermediate (N- and/or O-like species) is photoconverted back to the original resting state; thereby the long photocycle is cut short, giving rise to the large increase of the photostationary current. The results presented in this work indicate that the function to generate ion gradients across membranes is a general property of archaeal rhodopsins.

INTRODUCTION

The phototaxis of halophilic archaea is mediated by two receptors, the sensory rhodopsins I and II (SRI and SRII), which are responsible for positive and negative responses of the bacteria toward light (for a recent review see, e.g., Spudich, 1998). SRI and SRII are membrane proteins with seven transmembrane spanning helices and all-*trans* retinal bound to the opsin. On light excitation the archaeal sensory rhodopsins undergo a photocycle during which the physiological reaction is triggered. Sensory rhodopsins from *Halobacterium salinarum* have been sequenced (Blanck et al., 1989; Zhang et al., 1996) and in the case of the photophobic receptor also from the phylogenetically distinct *Natronobacterium pharaonis* (pSRII) (Seidel et al., 1995). The biochemical and physiological properties of pSRII are quite similar to those of SRII from *H. salinarum* as demonstrated in measurements of the photocycle (Scharf et al., 1992) and in their physiological response toward blue-green light (Scharf and Wolff, 1994). The signal transduction (reviewed in Marwan and Oesterhelt, 1999) is homologous to the eubacterial chemotactic so-called two-component system (reviewed in, e.g., Falke et al., 1997) in which the incoming signal triggers the activation of a cytoplasmic His kinase (CheA) from which the information is transferred to response regulators (e.g., CheY, CheB). Whereas the chemotactic receptors transfer an incoming signal directly to

their cytoplasmic domains, SRI and SRII form complexes with their corresponding transducers (halobacterial transducer of rhodopsin, Htr) (Ferrando-May et al., 1993; Lüttenberg et al., 1998; Sasaki and Spudich, 1998; Yao et al., 1994).

The amino acid sequence of the photophobic receptor pSRII is quite homologous to that of bacteriorhodopsin (BR) (Seidel et al., 1995). Residues involved in the proton release, such as Asp-85–BR or Arg-82–BR, are also present in the pSRII sequence. However, potentially charged amino acids such as Asp-96–BR, located in the cytoplasmic channel of the molecule, are not found. Furthermore, Asp residues on the cytoplasmic surface of BR are replaced by neutral amino acids in pSRII. Generally, the extracellular channels are quite homologous (with the exception of E194, which is replaced by P183 in pSRII). However, the cytoplasmic channel of pSRII has lost most of the amino acids that are known to facilitate the reprotonation of the Schiff base. Consequently, one can predict functional differences between the two pigments that are related to the second part of the reaction cycle. Indeed, a decreased rate of reprotonation of the Schiff base has been verified in recent work on the photocycle of pSRII (Chizhov et al., 1998).

Numerous publications on the mechanism of the proton pump in BR revealed the decisive participation of BR–Asp-85 and BR–Asp-96 in the proton transfer. These residues fulfill steering tasks, thereby increasing the photocycle turnover and the proton pump efficiency. Currently there is not a single mutant known that blocks the proton pump of BR entirely. Therefore, it is probable that the sensory rhodopsins can also pump protons. This has already been verified for SRI, although attached to its transducer the efficiency is abolished (Bogomolni et al., 1994; Spudich,

Received for publication 6 July 1999 and in final form 4 November 1999.

Address reprint requests to Dr. Martin Engelhard, Max-Planck-Institut für Molekulare Physiologie, Otto Hahn Strasse 11, D-44227 Dortmund, Germany. Tel.: 49-231-1332302; Fax: 49-231-1332399; E-mail: martin.engelhard@mpi-dortmund.mpg.de.

© 2000 by the Biophysical Society

0006-3495/00/02/967/10 \$2.00

1995) or at least reduced (Haupts et al., 1996). The capability to pump protons has not yet been rigorously proven for SRII or pSRII. According to Sasaki and Spudich (1999) SRII takes up a proton from the extracellular side during the $M \Rightarrow O$ transition and releases it concomitantly with the O -decay to the same side. This timing and location of proton transfer steps leads to a futile proton cycle. These data have to be reconciled to the observation that in pSRII Asp-75 is protonated probably by the proton of the Schiff base during the $L \Rightarrow M$ transition (Engelhard et al., 1996).

In the present work we describe the light-activated proton transfer reactions of pSRII and its channel-mutants D75N-pSRII and F86D-pSRII, which had been attached to black lipid membranes (BLM) (Bamberg et al., 1979). It can be shown that pSRII and F86D-pSRII can function as proton pumps and that the addition of external proton donors such as azide or imidazole increases the stationary photocurrent considerably.

MATERIALS AND METHODS

All reagents used were of analytical grade.

Expression in *H. salinarum*

For the expression of pSRII and its mutants in *H. salinarum* a strain (Pho81/w) was used whose genes for BR, HR, SRI, SRII, and the transducers *HtrI* and *HtrII* are defective (Olson and Spudich, 1993; Spudich and Spudich, 1993). Based on the shuttle vector pUSNovo, an expression vector pBL7Novo was designed in which the coding sequence of pSRII started downstream of the precursor sequence of *bop*, including the first two amino acids of the mature BR. *H. salinarum* Pho81/w was transformed essentially using the method of Cline and Doolittle (1987). The cells were spread on Novobiocin plates and positive clones were selected and subsequently genetically characterized by Southern blot analysis. A transformant containing a double insertion (probably by a double crossover event) of the *psp* gene into the *bop* gene locus (Pho81/wpSRII) was selected for the isolation of pSRII.

The *psopII* mutants (*psopII*-D75N; *psopII*-F86D) were prepared by PCR using the overlap-extension method (Higuchi et al., 1988; Ho et al., 1989). *Escherichia coli* cells were transformed by electroporation (Dower et al., 1988).

Expression in *E. coli*

For DNA manipulation *E. coli* strain XL1 was used. Gene expression was carried out in *E. coli* BL21 (DE3). The plasmid pET27bmod, derived from pET27b (Novagen, Madison, WI) was used to construct the expression vectors for the C-terminal 6x His-tagged pSOPII and F86DpSOPII genes. A detailed description of the cloning strategy for His-tagged pSOPII inserted between the 5'-*NcoI* and 3'-*HindIII* restriction sites is given in Shimono et al., 1998 and Hohenfeld et al., 1999. For the site-specific introduction of the F86D mutation extension-overlap PCR was used as described above (Ho et al., 1989). The His-tagged pSOPII gene was cloned into the pUCBM20 vector (Boehringer Mannheim, Germany) via *NcoI*/*HindIII* restriction. As a final PCR product the His-tagged pSOPII gene carrying the F86D mutation was ligated after restriction back into pET27bmod; pSRII and F86D-pSRII were expressed according to Shimono et al., 1998 and purified using the method of Hohenfeld et al., 1999.

Reconstitution into PM lipids

For reconstitution into native purple membrane lipids the solubilized proteins were shaken 16 h in a buffer (20 mM NaCl, 20 mM $\text{NaH}_2\text{PO}_4/\text{Na}_2\text{HPO}_4$, pH = 8.0) containing a 15-fold molar excess of lipids and detergent-adsorbing biobeads (Biorad München, Germany, SM2, 100 mg/mg protein). After filtration the reconstituted proteins were pelleted by centrifugation at $100,000 \times g$ (1 h, 4°C) and resuspended in 20 mM NaCl, $\text{NaH}_2\text{PO}_4/\text{Na}_2\text{HPO}_4$, pH = 7.5).

Laser flash photolysis

The laser flash photolysis setup and the data evaluation were essentially identical to those described by Chizhov et al., 1996. Laser flash-induced transient absorption was recorded at 20°C in the spectral range from 360 to 660 nm in steps of 10 nm. The experimental data were fitted using a multiexponential least-square fit procedure (Müller et al., 1991; Müller and Plesser, 1991).

Photocurrent measurements

Black lipid membranes with an area of 10^{-2} cm^2 were formed in a Teflon cell filled with the appropriate electrolyte solution (1.5 ml in each compartment). The membrane forming solution contained 1.5% (w/v) diphytanoyllecithin (Avanti Biochemicals, Birmingham, AL) and 0.025% (w/v) octadecylamine (Riedel-de Haen, Hannover, Germany) in *n*-decane to obtain a positively charged membrane surface (Dancshazy and Karvaly, 1976). Membrane formation was controlled by eye and the capacitance of each individual membrane was determined.

Membrane fractions containing pSRII or its mutants were suspended in distilled water and sonicated for 1 min in a sonication bath. Aliquots of 30 μl were added under stirring to the rear compartment of the cell containing the appropriate buffer. Photosensitivity (photocurrents) developed in time and reached a maximal and constant value after ~ 40 min. As light sources, a xenon lamp (100 W) or mercury lamp (100 W) were used. The intensity of the lamps in the plane of the membrane were 2 W/cm^2 and 4 W/cm^2 , respectively. Light reached the membrane after passing a heat protection filter. For "white" or "yellow" light cutoff filters $\lambda > 360 \text{ nm}$ or $\lambda > 495 \text{ nm}$ (Schott, Mainz, Germany) respectively, were used. A K40 broadband interference filter served for "blue" light excitation (maximal intensity: 2 W/cm^2). Light intensity was measured as described previously (Fendler et al., 1987). To obtain stationary currents the black lipid membrane was doped with the light-insensitive protonophores 1799 in combination with the Na^+ , K^+/H^+ exchanger monensin. Further details of the system were described earlier (Bamberg et al., 1979). It should be noted that the BLM experiments, which were done with both *E. coli*- and *H. salinarum*-expressed proteins, led to the same results.

RESULTS

Photocycle kinetics of pSRII, D75N-pSRII, and F86D-pSRII

Photocycle kinetics

In Fig. 1 the light-activated transient absorption changes of pSRII, F86D-pSRII, and D75N-pSRII are depicted at representative wavelengths. At 500 nm the depletion and reformation of the initial state of the pigments is monitored. The traces at 400 nm and 550 nm are indicative for the rise and decay of the M_{400} and O_{550} intermediates, respectively. The turnover rates of the photocycles of pSRII and F86D-

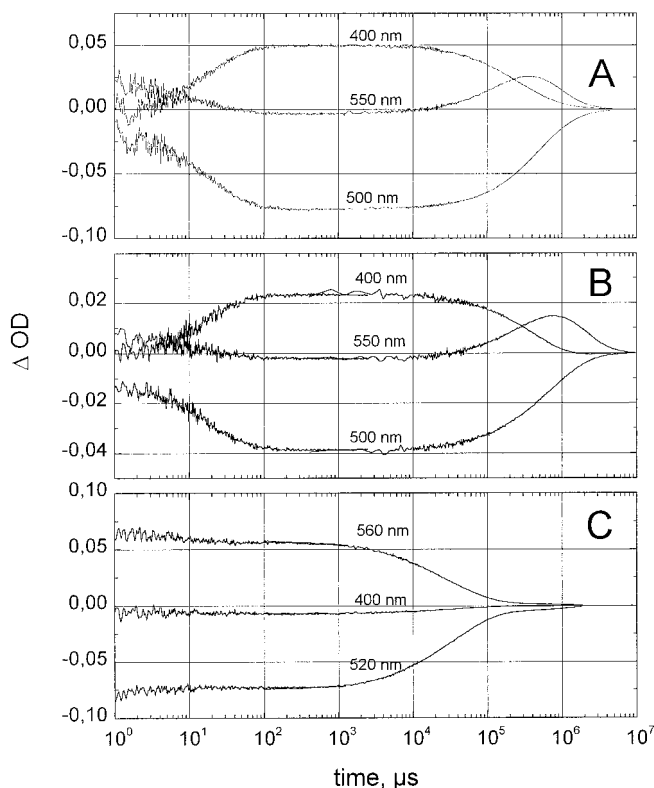


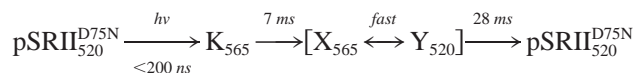
FIGURE 1 Photocycles of pSRII and the two channel mutants. The absorbance changes are depicted for 400, 500, and 550 nm (the traces for the D75N-pSRII mutant were measured at 400, 520, and 560 nm). These wavelengths are characteristic for the formation and decay of the M-, parent-, and O-state, respectively. (A) pSRII, (B) F86D-pSRII, (C) D75N-pSRII.

pSRII are quite similar and the reaction cycles are completed in the range of seconds. Compared with BR, this slow cycling rate reflects the physiological function of pSRII as a photoreceptor (for a detailed analysis of the pSRII photocycle see Chizhov et al., 1998). Whereas the deprotonation (M_{400} formation) is accomplished similarly to BR in $\sim 200 \mu\text{s}$, the second part, which depicts the reprotonation of the Schiff base, is slowed down by about two orders of magnitude.

Replacing in pSRII Phe-86 by Asp (F86D-pSRII) (Fig. 1 B) does not alter the photocycle kinetics (compare Fig. 1, A and B). This is corroborated by a global fit analysis of the photocycle kinetics of pSRII and the F86D mutant, which provides eight very similar components in both cases for a sufficient simulation to describe the experimental data (Ta-

ble 1). It should be noted that external conditions (e.g., solubilization, pH, and/or sample preparation) seem to influence the reprotonation and not the turnover rate. A faster protonation of the Schiff base has also been described by Kamo and co-workers using microsecond flash lamp excitation (Iwamoto et al., 1999).

The photochemical properties of pSRII drastically change when the primary acceptor group (Asp-75) of the proton from the Schiff base is replaced by the neutral Asn (Fig. 1 C). A consequence of this mutation is a shift of the absorption maximum from originally 500 nm to 522 nm. A similar bathochromic shift has been observed in other pigments as well, and is due to the neutralization of the Schiff base counterion (Chizhov et al., 1998; Zhu et al., 1997). Another effect of this mutation concerns the photocycle (Fig. 1 C). Faster than the dead time of the instrumental setup (200 ns), an intermediate appears which is stable over a time interval of ~ 10 ms. It decays back to the ground state with $\tau_2 = 28$ ms. No M-like intermediate could be detected. The global fit analysis and a modeling of the data to a scheme of irreversible first-order reactions reveals only two spectrally defined species (see Chizhov et al., 1996, 1998) for a detailed description of the data evaluation procedure). The first intermediate has an absorption maximum at 565 nm (Fig. 2 A) and decays with a half-life of $\tau_1 = 7$ ms. The product of this reaction absorbs maximally at 520 nm (Fig. 2 B). A shoulder is clearly visible on the long wavelength side of the absorption maximum. A Gaussian fit of the spectrum provides two species absorbing maximally at ~ 565 nm (X_{565}) and 520 nm (Y_{520}). The two peaks can be explained by a mixture of two rapidly equilibrating species. The rates of the forward and back reactions of this equilibrium must be fast compared with the rate of reformation ($\tau_2 = 28$ ms) of the original resting state. The photocycle of D75N-pSRII may then be described by the following scheme:



The two components X_{565} and Y_{520} can in principle be assigned to archetypical spectral states if data from further experimentation, e.g., Fourier transform infrared spectroscopy, become available. Taking the absorption maxima of the X_{565} and Y_{520} into account, one could assign the two species either to a $\text{K} \leftrightarrow \text{L}$ or an $\text{N} \leftrightarrow \text{O}$ equilibrium. Which of these assignments or other possibilities turns out to be

TABLE 1 Apparent half-times of pSRII, F86D-pSRII, and D75N-pSRII at 20°C (pH 7.5)

	τ_1	τ_2	τ_3	τ_4	τ_5	τ_6	τ_7	τ_8
pSRII	1 μs	17 μs	50 μs	1.5 ms	120 ms	300 ms	500 ms	1.5 s
F86D	1 μs	11 μs	36 μs	1.3 ms	90 ms	350 ms	570 ms	1.3 s
D75N-pSRII	<200 ns	7 ms	28 ms					

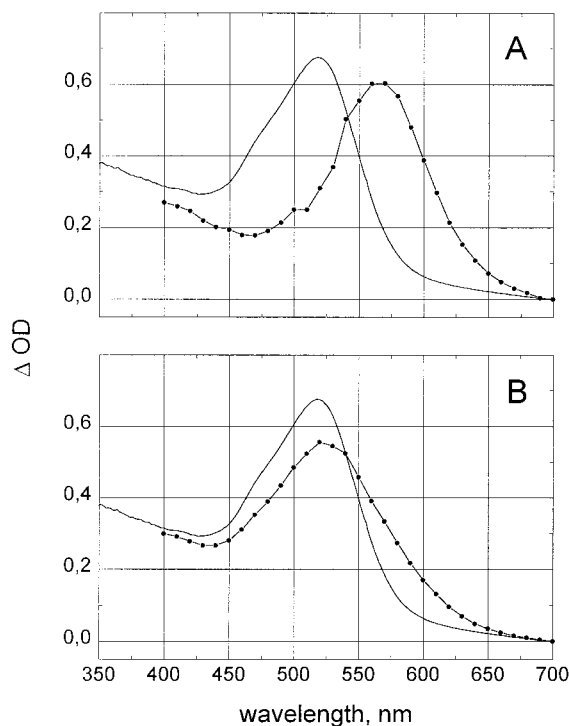


FIGURE 2 Photocycle of D75N-pSRII: absolute spectra of the two intermediates (solid line with dots). The spectra were derived from a global fit analysis of 31 wavelength scans from 360 to 660 nm (in steps of 10 nm). The method has been described in more detail in Chizhov et al. (1998). The first K-like ($\lambda_{\max} = 565$ nm) intermediate (A) decays with 7 ms into the N-like intermediate ($\lambda_{\max} = 510$ nm) (B). For comparison the spectrum of the original ground state is depicted (solid line) in each panel.

correct has to be seen. It should be noted that the thermal relaxations of the corresponding BR mutant (D85N-BR) proceed from K to L and N before reforming the initial state (Braiman et al., 1988; Needleman et al., 1991).

Effect of external proton donors on the photocycle kinetics of pSRII and F86D-pSRII

The transient absorption changes of pSRII at different concentrations of azide are illustrated in Fig. 3. As reported previously (Miyazaki et al., 1992; Takao et al., 1998) the experiments show that azide only accelerates the reprotonation of the Schiff base without having an influence on the M-formation or the overall turnover rate. Consequently, the decay of O_{550} denotes the rate-limiting step of the photocycle. The fast M-decay and the unaltered other rate constants are the reason for the accumulation of the O-intermediate at higher azide concentrations, as can be depicted from the traces at 550 nm. Similar results were obtained for the mutant F86D (data not shown). However, the BR mutant D96N-BR responds differently to azide. Not only the M-decay is significantly accelerated, but also the turnover rate (Tittor et al., 1989). It should be noted that the azide effect is pH-dependent (Takao et al., 1998). At a low pH ~ 4.7 ,

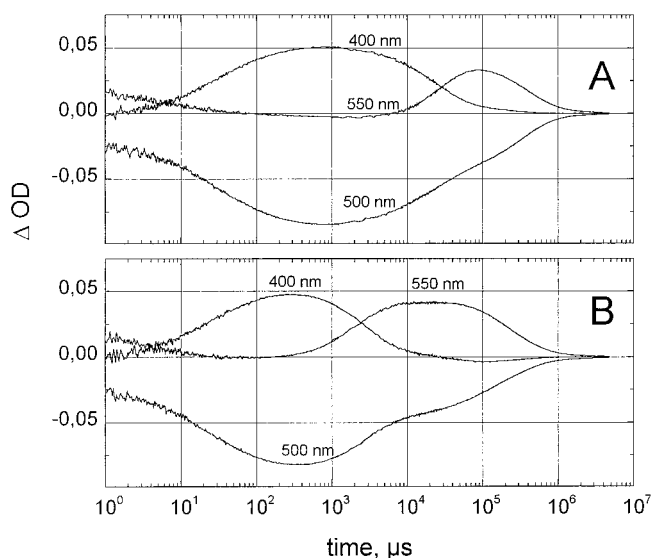
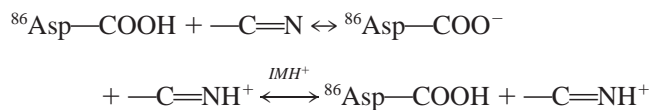


FIGURE 3 The effect of azide on the photocycle of pSRII. The absorbance changes were measured at 400, 500, and 550 nm at pH 7.5. (A) 100 mM azide; (B) 1 M azide.

azide enhances the reprotonation of the Schiff base, indicating that HN_3 rather than N_3^- is the active species.

The M-decay of the F86D mutant is not only accelerated by azide, but also by imidazole. The corresponding traces are not shown because they are quite similar to those observed for azide (Fig. 3). The response of F86D-pSRII toward imidazole accidentally observed in the course of its purification has been unforeseen, especially in light of the effect on pSRII and D75N-pSRII, which are not influenced at all (data not shown). The reason for these differences is not known. However, there are at least two possible explanations. Imidazole, like azide, is a weak proton donor, but the different size, steric properties, and polarity might hinder imidazole to have a cytoplasmic access to the Schiff base in the wild-type but not in the F86D mutant. A second possibility could be that imidazole (IMH^+) specifically interacts with Asp-86 by catalyzing (e.g., altering the pK_a) its reprotonation, thereby shifting the equilibria



toward the right. Which of these two possibilities turns out to be correct remains open.

Interestingly, Zhang and Spudich (1997) reported a similar observation for SRI from *H. salinarum*. Imidazole also had no influence on the decay of the SRI₃₇₃ (M)-intermediate, but the M-decay of the H166A mutant is 10-fold, accelerated upon the addition of 10 mM imidazole. The authors conclude that His-166 plays a critical role in the protonation pathways of SRI and therefore imidazole might

mimic His-66. However, in pSRII the corresponding residue (Leu) is not conserved, which points to a more direct participation of imidazole in the proton transfer process.

Photocurrent measurements of pSRII, D75N-pSRII, and F86D-pSRII

Photocurrent measurements of pSRII and D75N-pSRII

The photocurrents (excitation wavelength $\lambda > 495$ nm, green) of pSRII are shown in Fig. 4 at different conditions. At neutral pH (Fig. 4 A) only a transient downward deflection can be detected, which corresponds to a movement of positive charges toward the protein-free side of the BLM. It is the same direction as that observed for BR (Fahr et al.,

1981) or D96N-BR (Tittor et al., 1989), which indicates (assuming a preferential attachment of the extracellular side of pSRII to the BLM, as was found for BR) that the charge displacement has the same vectoriality in BR and pSRII, namely from the cytoplasm to the external medium. The sign of the transient current is in agreement with the deprotonation of the Schiff base (formation of M) and the protonation of Asp-75. At this pH no photostationary current is observed.

Decreasing the pH to 4.7 results in a small but distinct stationary photocurrent (Fig. 4 B) of ~ 0.6 nA/cm² which could reflect, compared with pSRII at pH 6.8 (Fig. 4 A), an accelerated turnover rate. In previous work it has been shown that between pH 9 and pH 6 the photocycle of pSRII is pH-independent (Chizhov et al., 1998; see Table 1 for the photocycle data at pH 6.8). Also, the kinetic data at pH 5.5 are almost identical, with the exception of τ_7 (O-decay), which decreases by a factor of 2. Unfortunately, the evaluation of the photocycle data at lower pH values is impaired because Asp-75 becomes protonated ($pK_a = 5.6$), which leads to a photocycle (data not shown) similar to that of the mutant D75N-pSRII (see above). Taking the decrease of τ_7 between pH 6 and pH 5.5 into account, it seems likely that a further increase in the turnover rate at lower pH 4.7 is responsible for the observed small stationary photocurrent, though the concentration of active species is reduced.

The above considerations imply that at pH 4.7 two species are photoactivated and may contribute to the transient and/or stationary photocurrent. This is substantiated by a closer inspection of the transient photocurrent. As can be seen from Fig. 4 B the onset of the transient photocurrent is a superposition of two signals of opposite sign, which is not seen for pSRII at pH 6.8 (Fig. 4 A), indicating the presence of at least two species. The upward deflection corresponds to the transient current obtained with the mutant D75N (Fig. 4 D).

The stationary photocurrent of the pSRII wild type can be considerably enhanced by the addition of azide (30 mM) and reaches values of ~ 40 nA/cm² (Fig. 4 C). A 10-fold increase of the steady-state signal can already be observed at a concentration of 1 mM azide, and saturates at 50–100 mM azide with an ≈ 70 -fold larger amplitude. From this saturation curve an apparent binding constant can be estimated ($K_m = 7$ mM). A similar increase of the steady-state photocurrent is also measured at higher pH values, though for the same enlargement the azide concentration has to be increased.

Replacement of Asp-75 as the acceptor for the Schiff base proton by Asn inverts the direction of the transient photocurrent (Fig. 4 D), whereas a photostationary current was not observed. The corresponding BR mutant D85N (Ganea et al., 1998; Tittor et al., 1995) and SRI (Haupts et al., 1996), when illuminated with red light (>630 nm), similarly display transient photocurrents that are directed toward the cytoplasmic side. However, in contrast to the

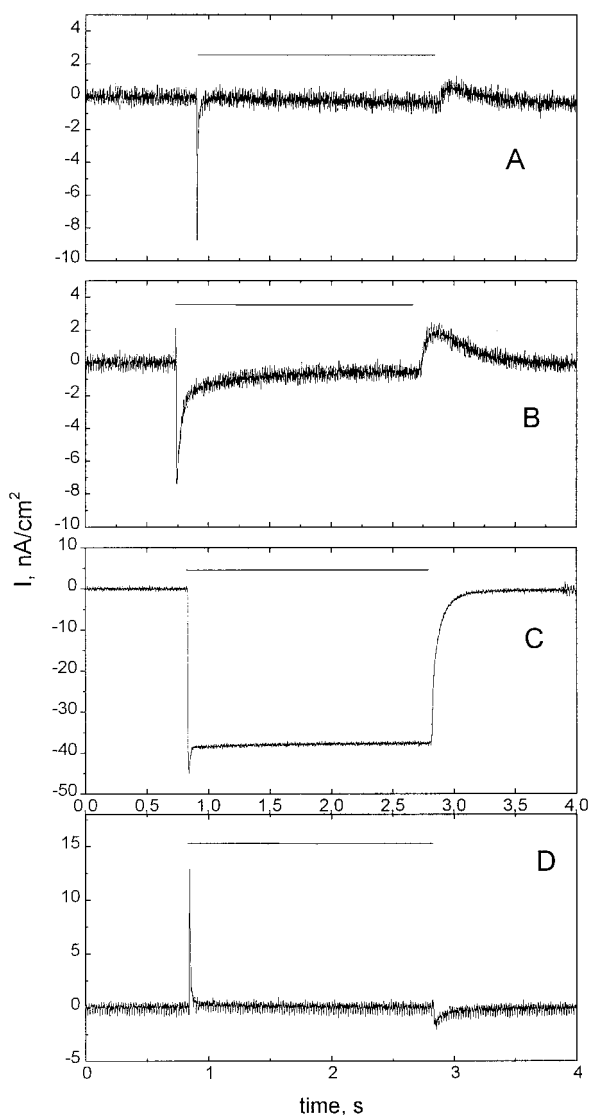


FIGURE 4 Photocurrent of pSRII at different pH values (A, pH 6.8; B, pH 4.7) and in the presence of 30 mM azide (C). In (D) the photocurrent of the D75N-pSRII mutant at pH 4.5 is depicted. The bars above the traces indicate the illumination period ($\lambda > 495$ nm).

D85N-BR mutant, D75N-pSRII responses quite different to blue light in the presence of azide (100 mM azide at pH 4.7). Under these conditions a very small inwardly directed photostationary current develops and not, as observed for the BR-mutant, an outwardly directed charge movement. This former observation has also been described for SRI₅₉₀, which can be selectively excited by red light (Haupts et al., 1996).

In pSRII typical blue-light quenching of the photocurrent is observed (Fig. 5 A) which is much better resolved in the presence of 10 mM azide (Fig. 5 B). This inhibition of the proton transfer has originally been described in BR and has

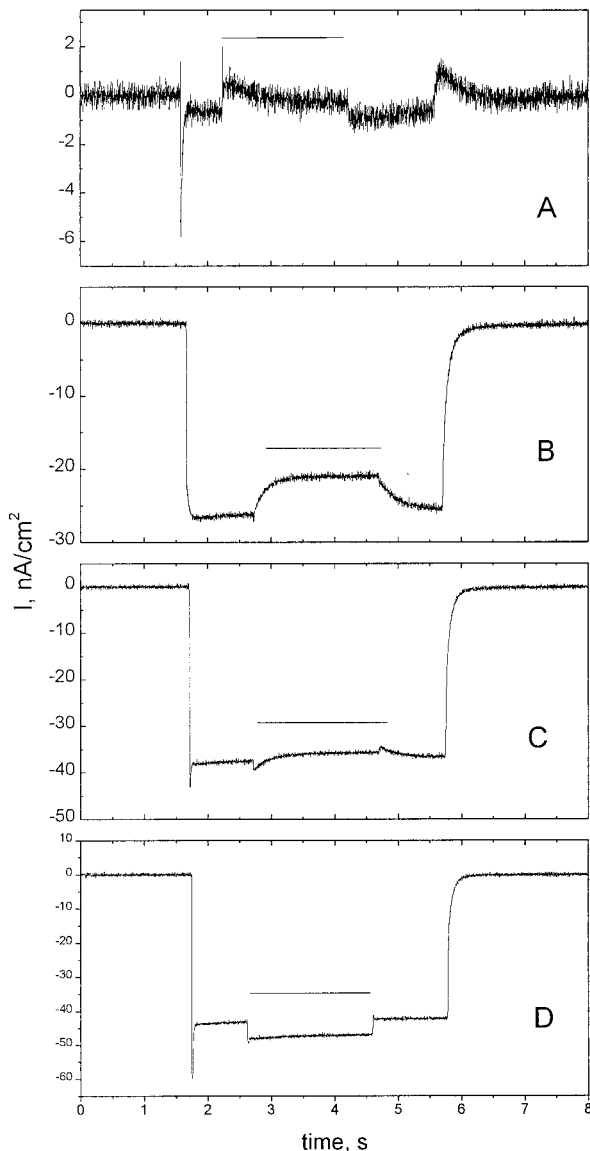


FIGURE 5 The effect of blue light on the photocurrent of pSRII at pH 4.8. The bar above the four panels indicate the illumination with orange light ($\lambda > 495$ nm). The additional irradiation of the sample with blue light ($\lambda = 380\text{--}420$ nm) is depicted by the bars above the individual traces. (A) no azide, (B) 10 mM azide, (C) 50 mM azide, (D) 100 mM azide.

been explained by the photoexcitation of the M-intermediate with a second photon that short-circuits the proton pumping cycle (Ormos et al., 1978). Control experiments at pH 6.8 with the addition of azide gave similar results (data not shown). These experiments clearly demonstrate that pSRII, like BR, functions as an outward-directed proton pump. As in BR, the long-lived M-intermediate can be photochemically reverted back to the initial ground state, resulting in an inhibition of the photostationary current.

The quenching of the photostationary current of pSRII by blue light is dependent on the azide concentration. With increasing amounts of azide the inhibition is first diminished so that at $\sim 30\text{--}50$ mM only the fast transient signal can be observed (Fig. 5 C). Subsequently, an enhancement of the photocurrent by the additional blue light is observed (Fig. 5 D). At ~ 100 mM azide the surplus photocurrent saturates. One possible explanation for this positive effect might be that the M-decay is accelerated by higher azide concentrations, which would lead to smaller steady-state M concentrations. It follows that blue light (K 40 filter, $\lambda = 380\text{--}420$ nm) becomes more and more inefficient for quenching. The absorption spectrum of pSRII has considerable extinction in this region (Chizhov et al., 1998) so that its photocycle can also be triggered by blue light. Since the flux of photons is constant throughout the experiments, these two effects could result in an enhancement of the photostationary current by blue light.

Photocurrent of the mutant F86D-pSRII

The photocurrent measurements of F86D-pSRII are shown in Fig. 6. At neutral pH illumination of the sample with green light generates an outwardly directed transient current that is followed by a stationary current in the same direction (Fig. 6 A). The signal unequivocally proves that the incorporation of a carboxyl group into the cytoplasmic channel (Asp in position 86) is sufficient to generate proton pump activity.

The addition of azide to the sample chamber increases the transient and stationary current considerably, as it has also been observed for the wild-type protein (Fig. 4 C). Interestingly, imidazole has a similar effect (Fig. 6 C) which is not observed for pSRII. Taking the photocycle data into account, these results are surprising because the turnover rates do not differ from those of the wild type.

DISCUSSION

The amino acid sequence of pSRII is quite similar to that of BR, however notable exceptions are especially found in the cytoplasmic proton channel. Taking recent x-ray diffraction data of BR (Belrhali et al., 1999; Essen et al., 1998; Luecke et al., 1999; Pebay-Peyroula et al., 1997) into account, it is obvious that residues of the cytoplasmic proton pathway are not found in pSRII. From five polar residues possibly in-

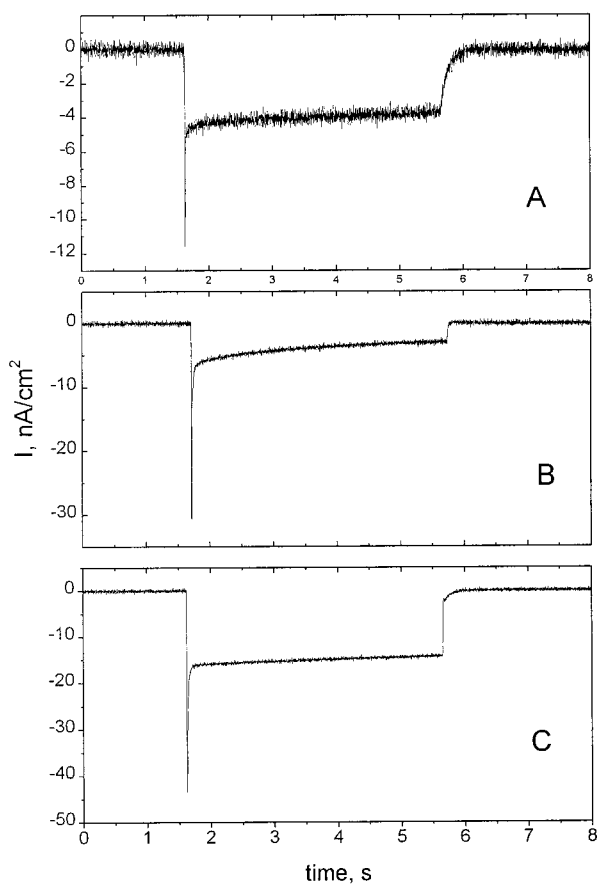


FIGURE 6 Photocurrent of F86D-pSRII (A) and in the presence of 50 mM imidazole (B) and 50 mM imidazole/50 mM azide (C) at pH 6.8. The sample was irradiated with orange light (solid bar above the three panels).

involved in proton transfer only three are altered to neutral amino acids, namely D38, T46, and D96. However, residues of the extracellular channel are almost all (with the notable exception of E194) conserved. The photocycle data of wild-type pSRII clearly reflect this pattern (see Table 1; Chizhov et al., 1998). A similar behavior is found in BR mutants in which Asp-96 is replaced by a neutral amino acid (e.g., D96N-BR; Tittor et al., 1989). Although the time courses are quite similar, the reformations of the ground states are following different pathways. Whereas in D96N-BR the M-decay is greatly simplified without any transient accumulation of N and O species (Nagle et al., 1995; Zimányi et al., 1999), these latter intermediates can readily be detected in pSRII (Chizhov et al., 1998).

Comparing the response of pSRII and D96N-BR toward azide, another striking difference becomes apparent. Although azide catalyzes the reprotonation of the Schiff base in D96N-BR as well as in pSRII, the reformation of the original ground state is not accelerated in the latter pigment. Moreover, as is apparent at increasing azide concentrations, the reprotonation of the Schiff base is considerably accelerated. However, reactions within the protein that finally

lead back to the resting state are not at all influenced. Obviously, the positive charge of the Schiff base seems to influence neither the kinetics of the *cis-trans* isomerization of retinal or the deprotonation of Asp-75, which is still protonated in the O-intermediate (F. Siebert, personal communication) nor the timing of conformational changes that restore the original ground state of pSRII. Another trigger has to reestablish the initial state. Such a crucial step could be, e.g., the deprotonation of Asp-75. It should be noted that the analogous SRII mutant from *H. salinarum* is constitutively active (Spudich et al., 1997). Taking these data into account, one could speculate that the neutralization of Asp-75 is an important factor to produce the signaling state of the photophobic receptor. It will be interesting to analyze the charge transfer properties of this SRII mutant and to study the physiological properties of D75N-pSRII.

At pH 6.8 a stationary photocurrent, as was demonstrated for BR under the same conditions, cannot be detected for pSRII. Taking the amplitude of the transient signal into account, it can be excluded that the absence of a steady-state photocurrent is due to a low number of active cycling proteins. Generally, the size of a photostationary current is dependent on the turnover number of the ion pump (Fahr et al., 1981). In BR a photostationary current of ~ 100 nA/cm² has been measured. Taking the turnover numbers of BR and pSRII into account one could expect a photocurrent of ~ 1 nA/cm² for pSRII, which is close to the detection limit of the system. Similarly, for D96N-BR, whose monophasic M-decay is ~ 500 ms, almost no photostationary current has been found (Tittor et al., 1989).

Lowering the pH to 4.7 establishes a small but distinct photostationary current. It has already been mentioned that at lower pH the absorption maximum of pSRII shifts from 500 to 520 nm, forming a "pink" membrane, which gives rise to the inwardly directed transient photocurrent. It is therefore unlikely that the "pink" membrane can also transfer protons from the inside to the outside of the cell. It follows that at pH 4.7 only few active species ($<25\%$) of pSRII could contribute to the photostationary current. These active species must have a high turnover number to generate the stationary current. As was shown above, a decrease of the pH from pH 6 to pH 5.5 accelerates the reformation of the initial state by at least a factor of two. Under the assumption that a further increase of the proton concentration (pH 4.7) would additionally shorten the photocycle turnover, the observed stationary photocurrent can be explained. In conclusion, the data of the photostationary and transient currents indicate that pSRII, like D96N-BR, is an outward-directed proton pump.

The kinetic data (Figs. 1 and 3) demonstrated that external proton donors such as azide or imidazole increase the rate of the reprotonation of the Schiff base although the overall duration of the photocycle has not changed. Because the rate-limiting steps in the catalytic cycle are not considerably affected, a photostationary current should not be

observed. The discrepancy between photocycle data and the presence of a photostationary current in pSRII (in the presence of azide) and F86D-pSRII poses a problem because the proton pump activity is obviously not dependent on the slow photocycle turnover.

A conceivable mechanism for the proton pump activity of pSRII in the presence of azide and that of F86D-pSRII might be that the reprotonation of the Schiff base can occur from both the extracellular and cytoplasmic channel. This model would imply that although the photocycle turnover is quite slow, the Schiff base in the wild type is reprotonated from the extracellular side. The mutation from Phe to Asp in F86D-pSRII, azide, or lowering the pH (assuming that increasing proton concentrations only affect the reprotonation rate of the Schiff base from the cytoplasmic, but not the extracellular channel) would facilitate protonation of the Schiff base from the cytoplasmic channel (fast equilibrium between two M intermediates; local access model? (Brown et al., 1998)), thereby increasing the photostationary current. The photostationary currents measured in the presence of azide would represent maximal output governed by the photocycle turnover. However, at neutral pH the reprotonation of the Schiff base would occur in pSRII from the extracellular channel, thus being unable to generate a photostationary current. Recent experiments that support this model indicate that the uptake of protons from the bulk medium (during the $M \Rightarrow O$ transition) precedes the release of protons (Sasaki and Spudich, 1999; N. Kamo, personal communication). Furthermore, Sasaki and Spudich (1999) provide evidence that the proton uptake and release both occur from the same extracellular side. This observation could explain why a photostationary current could not be observed in wild-type pSRII at pH 6.8.

The photocurrent results could also be explained by a two-photon process. Whereas the measurements of the photocycle are single-turnover experiments, the photocurrent is determined under constant illumination (excitation wavelength > 495 nm) of the protein. The (photo) steady-state mixture of pSRII consists mainly of the M intermediate (Engelhard et al., 1996), which absorbs maximally at 390 nm (Chizhov et al., 1998) and is therefore unable to absorb the second photon. However, if the addition of azide or the mutation F86D would shift the photo-steady-state mixture toward the N- and O-intermediates that appear later in the photocycle and have considerable absorption at wavelengths above 495 nm, a two-photon process would become possible. Excitation of the N- and/or O-intermediate would accelerate the photocycle considerably and the turnover could reach the millisecond range. A similar two-photon process in pSRII at pH 6.8 cannot be excluded. However, under these conditions the steady-state concentration of N and O is apparently too low (Engelhard et al., 1996) to contribute significantly to the photostationary current.

These assumptions are corroborated in preliminary flash photolysis experiments on background-illuminated (white

TABLE 2 Conditions for generating photocurrents in pSRII and its mutants

	Mixture of photostationary state	Number of photons	Photocurrent*	Direction
pSRII (pH 4.7)	M_{400}^{\ddagger}	1	+	outward
pSRII + azide	$M_{400} + N, O^{\ddagger}$	2	+++	outward
F86D	$M_{400} + N, O^{\ddagger}$	2	++	outward
D75N + azide	K, N^{\ddagger}	1	+	inward

*+, small; ++, medium; +++, large.

[†]Engelhard et al., 1996.

[‡]F. Siebert, personal communication; see text.

light) samples of pSRII and F86D-pSRII at neutral pH. Under these conditions the steady-state concentration of at least the O-intermediate is significantly increased. Additional measurements of FTIR-spectra of pSRII in the presence of azide and of F86D-pSRII under continuous illumination clearly indicate that the steady-state mixtures of both samples contain species with a protonated Schiff base (F. Siebert, personal communication). These data are in line with two-photon processes to explain the proton pump activities of pSRII and its F86D mutant (Table 2). It is interesting to note that the switch separating the cytoplasmic from the extracellular accessibility of the Schiff base must have occurred before the second photon was absorbed. Otherwise, an inhibition of the photocurrent should have been observed.

The two explanations for the photocurrent behavior of pSRII are not exclusive. It could be possible that mechanism I (proton uptake and release from the same side) holds for wild-type pSRII at neutral pH, whereas mechanism II (two-photon process) is valid in cases where external and/or internal proton donors are present.

We thank M. Kolleck for excellent technical assistance.

The work was supported by Deutsche Forschungsgemeinschaft Grants En87 10-2 (to M.E.) and SFB 479 (to E.B.). G.S gratefully acknowledges a fellowship by the Boeringer Ingelheim Fonds.

REFERENCES

- Bamberg, E., H.-J. Apell, N. A. Dencher, W. Sperling, H. Stieve, and P. Luger. 1979. Photocurrents generated by bacteriorhodopsin on planar bilayer membranes. *Biophys. Struct. Mech.* 5:277–292.
- Belrhali, H., P. Nollert, A. Royant, C. Menzel, J. P. Rosenbusch, E. M. Landau, and E. Pebay-Peyroula. 1999. Protein, lipid and water organization in bacteriorhodopsin crystals: a molecular view of the purple membrane at 1.9 Å resolution. *Structure*. 7:909–917.
- Blanck, A., D. Oesterhelt, E. Ferrando, E. S. Schegk, and F. Lottspeich. 1989. Primary structure of sensory rhodopsin I, a prokaryotic photoreceptor. *EMBO J.* 8:3963–3971.
- Bogomolni, R. A., W. Stoeckenius, I. Szundi, E. Perozo, K. D. Olson, and J. L. Spudich. 1994. Removal of transducer HtrVI allows electrogenic proton translocation by sensory rhodopsin I. *Proc. Natl. Acad. Sci. USA.* 91:10188–10192.

- Braiman, M. S., T. Mogi, T. Marti, L. J. Stern, H. G. Khorana, and K. J. Rothschild. 1988. Vibrational spectroscopy of bacteriorhodopsin mutants: light-driven proton transport involves protonation changes of aspartic acid residues 85, 96, and 212. *Biochemistry*. 27:8516–8520.
- Brown, L. S., A. K. Dioumaev, R. Needleman, and J. K. Lanyi. 1998. Connectivity of the retinal Schiff base to Asp-85 and Asp-96 during the bacteriorhodopsin photocycle: the local-access model. *Biophys. J.* 75:1455–1465.
- Chizhov, I., D. S. Chernavskii, M. Engelhard, K. H. Müller, B. V. Zubov, and B. Hess. 1996. Spectrally silent transitions in the bacteriorhodopsin photocycle. *Biophys. J.* 71:2329–2345.
- Chizhov, I., G. Schmies, R. Seidel, J. R. Sydor, B. Lüttenberg, and M. Engelhard. 1998. The photophobic receptor from *Natronobacterium pharaonis*: temperature and pH dependencies of the photocycle of sensory rhodopsin II. *Biophys. J.* 75:999–1009.
- Cline, S. W., and F. Doolittle. 1987. Efficient transfection of the Archaeobacterium *Halobacterium halobium*. *J. Bacteriol.* 169:1341–1344.
- Dancshazy, Z., and B. Karvaly. 1976. Incorporation of bacteriorhodopsin into a bilayer lipid membrane; a photoelectric-spectroscopic study. *FEBS Lett.* 72:136–138.
- Dower, W. J., J. F. Miller, and C. W. Ragsdale. 1988. High efficiency transformation of *E. coli* by high voltage electroporation. *Nucleic Acids Res.* 16:6127–6145.
- Engelhard, M., B. Scharf, and F. Siebert. 1996. Protonation changes during the photocycle of sensory rhodopsin II from *Natronobacterium pharaonis*. *FEBS Lett.* 395:195–198.
- Essen, L. O., R. Siebert, W. D. Lehmann, and D. Oesterhelt. 1998. Lipid patches in membrane protein oligomers: crystal structure of the bacteriorhodopsin-lipid complex. *Proc. Natl. Acad. Sci. USA.* 95:11673–11678.
- Fahr, A., P. Läger, and E. Bamberg. 1981. Photocurrent kinetics of purple-membrane sheets bound to planar bilayer membranes. *J. Membr. Biol.* 60:51–62.
- Falke, J. J., R. B. Bass, S. L. Butler, S. A. Chervitz, and M. A. Danielson. 1997. The two-component signaling pathway of bacterial chemotaxis: a molecular view of signal transduction by receptors, kinases, and adaptation enzymes. *Annu. Rev. Cell Dev. Biol.* 13:457–512.
- Fendler, K., W. Gärtner, D. Oesterhelt, and E. Bamberg. 1987. Electromagnetic transport properties of bacteriorhodopsin containing chemically modified retinal analogues. *Biochim. Biophys. Acta.* 893:60–68.
- Ferrando-May, E., M. Krahe, W. Marwan, and D. Oesterhelt. 1993. The methyl-accepting transducer protein HtrI is functionally associated with the photoreceptor sensory rhodopsin I in the archaeon *Halobacterium salinarium*. *EMBO J.* 12:2999–3005.
- Ganea, C., J. Tittor, E. Bamberg, and D. Oesterhelt. 1998. Chloride- and pH-dependent proton transport by BR mutant D85N. *Biochim. Biophys. Acta.* 1368:84–96.
- Haupts, U., E. Bamberg, and D. Oesterhelt. 1996. Different modes of proton translocation by sensory rhodopsin I. *EMBO J.* 15:1834–1841.
- Higuchi, R., B. Krummel, and R. K. Saiki. 1988. A general method of in vitro preparation and specific mutagenesis of DNA fragments: study of protein and DNA interactions. *Nucleic Acids Res.* 7351–7367.
- Ho, S. N., H. D. Hunt, R. M. Horton, J. K. Pullen, and L. R. Pease. 1989. Site-directed mutagenesis by overlap extension using the polymerase chain reaction. *Gene.* 77:51–59.
- Hohenfeld, I. P., A. A. Wegener, and M. Engelhard. 1999. Purification of histidine-tagged bacteriorhodopsin, *pharaonis* halorhodopsin and *pharaonis* sensory rhodopsin II functionally expressed in *Escherichia coli*. *FEBS Lett.* 442:198–202.
- Iwamoto, M., K. Shimono, M. Sumi, and N. Kamo. 1999. Positioning proton-donating residues to the Schiff-base accelerates the M-decay of *pharaonis* phoborhodopsin expressed in *Escherichia coli*. *Biophys. Chem.* 79:187–192.
- Luecke, H., B. Schobert, H. T. Richter, and J. K. Lanyi. 1999. Structure of bacteriorhodopsin at 1.55 Å resolution. *J. Mol. Biol.* 291:899–911.
- Lüttenberg, B., E. K. Wolff, and M. Engelhard. 1998. Heterologous coexpression of the blue light receptor pSRII and its transducer pHtrII from *Natronobacterium pharaonis* in the *Halobacterium salinarium* strain pho81/w restores negative phototaxis. *FEBS Lett.* 426:117–120.
- Marwan, W., and D. Oesterhelt. 1999. Archaeal vision and bacterial smelling: sensory control of the swimming behavior by two-component signaling and fumarate. *ASM-News*. In press.
- Miyazaki, M., J. Hirayama, M. Hayakawa, and N. Kamo. 1992. Flash photolysis study on *pharaonis* phoborhodopsin from a haloalkaliphilic bacterium (*Natronobacterium pharaonis*). *Biochim. Biophys. Acta.* 1140:22–29.
- Müller, K.-H., H. J. Butt, E. Bamberg, K. Fendler, B. Hess, F. Siebert, and M. Engelhard. 1991. The reaction cycle of bacteriorhodopsin: an analysis using visible absorption, photocurrent and infrared techniques. *Eur. Biophys. J.* 19:241–251.
- Müller, K.-H., and Th. Plesser. 1991. Variance reduction by simultaneous multi-exponential analysis of data sets from different experiments. *Eur. Biophys. J.* 19:231–240.
- Nagle, J. F., L. Zimányi, and J. K. Lanyi. 1995. Testing BR photocycle kinetics. *Biophys. J.* 68:1490–1499.
- Needleman, R., M. Chang, B. Ni, G. Váró, J. Fornés, S. H. White, and J. K. Lanyi. 1991. Properties of Asp²¹² → Asn bacteriorhodopsin suggest that Asp²¹² and Asp⁸⁵ both participate in a counterion and proton acceptor complex near the Schiff base. *J. Biol. Chem.* 266:11478–11484.
- Olson, K. D., and J. L. Spudich. 1993. Removal of the transducer protein from sensory rhodopsin I exposes sites of proton release and uptake during the receptor photocycle. *Biophys. J.* 65:2578–2585.
- Ormos, P., Z. Dancshazy, and B. Karvaly. 1978. Mechanism of generation and regulation of photopotential by bacteriorhodopsin in bimolecular lipid membrane. *Biochim. Biophys. Acta.* 503:304–315.
- Pebay-Peyroula, E., G. Rummel, J. P. Rosenbusch, and E. M. Landau. 1997. X-ray structure of bacteriorhodopsin at 2.5 Å resolution from microcrystals grown in lipidic cubic phases. *Science.* 277:1676–1681.
- Sasaki, J., and J. L. Spudich. 1998. The transducer protein HtrII modulates the lifetimes of sensory rhodopsin II photointermediates. *Biophys. J.* 75:2435–2440.
- Sasaki, J., and J. L. Spudich. 1999. Proton circulation during the photocycle of sensory rhodopsin II. *Biophys. J.* 77:2145–2152.
- Scharf, B., B. Pevec, B. Hess, and M. Engelhard. 1992. Biochemical and photochemical properties of the photophobic receptors from *Halobacterium halobium* and *Natronobacterium pharaonis*. *Eur. J. Biochem.* 206:359–366.
- Scharf, B., and E. K. Wolff. 1994. Phototactic behaviour of the archaeobacterial *Natronobacterium pharaonis*. *FEBS Lett.* 340:114–116.
- Seidel, R., B. Scharf, M. Gautel, K. Kleine, D. Oesterhelt, and M. Engelhard. 1995. The primary structure of sensory rhodopsin II: a member of an additional retinal protein subgroup is coexpressed with its transducer, the halobacterial transducer of rhodopsin II. *Proc. Natl. Acad. Sci. USA.* 92:3036–3040.
- Shimono, K., M. Iwamoto, M. Sumi, and N. Kamo. 1998. V108M mutant of *pharaonis* phoborhodopsin: substitution caused no absorption change but affected its M-state. *J. Biochem.* 124:404–409.
- Spudich, J. L. 1995. Transducer protein HtrI controls proton movements in sensory rhodopsin I. *Biophys. Chem.* 56:165–169.
- Spudich, J. L. 1998. Variations on a molecular switch: transport and sensory signaling by archaeal rhodopsins. *Mol. Microbiol.* 28:1051–1058.
- Spudich, E. N., and J. L. Spudich. 1993. The photochemical reactions of sensory rhodopsin I are altered by its transducer. *J. Biol. Chem.* 268:16095–16097.
- Spudich, E. N., W. S. Zhang, M. Alam, and J. L. Spudich. 1997. Constitutive signaling by the phototaxis receptor sensory rhodopsin II from disruption of its protonated Schiff base Asp-73 interhelical salt bridge. *Proc. Natl. Acad. Sci. USA.* 94:4960–4965.
- Takao, K., T. Kikukawa, T. Arais, and N. Kamo. 1998. Azide accelerates the decay of M-intermediate of *pharaonis* phoborhodopsin. *Biophys. Chem.* 73:145–153.
- Tittor, J., D. Oesterhelt, and E. Bamberg. 1995. Bacteriorhodopsin mutants D85N, D85T and D85,96N as proton pumps. *Biophys. Chem.* 56:153–157.

- Tittor, J., C. Soell, D. Oesterhelt, H.-J. Butt, and E. Bamberg. 1989. A defective proton pump, point-mutated bacteriorhodopsin Asp96 → Asn is fully reactivated by azide. *EMBO J.* 8:3477–3482.
- Yao, V. J., E. N. Spudich, and J. L. Spudich. 1994. Identification of distinct domains for signaling and receptor interaction of the sensory rhodopsin I transducer, HtrI. *J. Bacteriol.* 176:6931–6935.
- Zhang, W. S., A. Brooun, M. M. Mueller, and M. Alam. 1996. The primary structures of the archaeon *Halobacterium salinarium* blue light receptor sensory rhodopsin II and its transducer, a methyl-accepting protein. *Proc. Natl. Acad. Sci. USA.* 93:8230–8235.
- Zhang, X. N., and J. L. Spudich. 1997. His-166 is critical for active-site proton transfer and phototaxis signaling by sensory rhodopsin I. *Biophys. J.* 73:1516–1523.
- Zhu, J. Y., E. N. Spudich, M. Alam, and J. L. Spudich. 1997. Effects of substitutions D73E, D73N, D103N and V106M on signaling and pH titration of sensory rhodopsin II. *Photochem Photobiol.* 66:788–791.
- Zimányi, L., A. Kulcsár, J. K. Lanyi, D. F. J. Sears, and J. Saltiel. 1999. Intermediate spectra and photocycle kinetics of the Asp96 → Asn mutant bacteriorhodopsin determined by singular value decomposition with self-modeling. *Proc. Natl. Acad. Sci. USA.* 96:4414–4419.